Journal of Hazardous Materials 192 (2011) 1370–1379

Contents lists available at ScienceDirect

Journal of Hazardous Materials

journal homepage: www.elsevier.com/locate/jhazmat

Adsorption of toluene, ethylbenzene and m-xylene on multi-walled carbon nanotubes with different oxygen contents from aqueous solutions

Fei Yu[a], Jie Ma[b], Yanqing Wu[a,*]

[a] School of Environmental Science and Engineering, Shanghai Jiao Tong University, Shanghai 200240, China
[b] State Key Laboratory of Pollution Control and Resource Reuse, School of Environmental Science and Engineering, Tongji University, Shanghai 200092, China

ARTICLE INFO

Article history:
Received 20 February 2011
Received in revised form 29 May 2011
Accepted 18 June 2011
Available online 20 July 2011

Keywords:
Adsorption
TEX
Multi-walled carbon nanotube
Surface oxygen content

ABSTRACT

The purified and oxidized multi-walled carbon nanotubes (MWCNTs) with different oxygen contents are employed as adsorbents to study their physicochemical properties and adsorption behaviors of toluene, ethylbenzene and m-xylene (TEX) in aqueous solutions. The results demonstrate that adsorption capacity is significantly enhanced for 3.2% surface oxygen, but is dramatically reduced for 5.9% oxygen concentration. The adsorption kinetics is investigated and fitted with pseudo-second-order model. The adsorption isotherms are found to be fitted with Langmuir model. More interestingly, with the increasing of surface oxygen content, maximum adsorption capacities firstly increased, and then, began to decrease. In the first stage, dispersion is the most important factor. A better dispersive interaction increases the available adsorption sites, which consequently can be favorable for the aqueous phase adsorption. Therefore, maximum adsorption capacity is remarkably enhanced with the increasing of oxygen content, which is according with our results. However, in the second stage, when oxygen content increases to a certain extent, hydroxyl groups cause water clusters formation on the surface or tube end of MWCNTs, which hinder the interaction between TEX and MWCNTs. Consequently, more oxygen content leads to the decrease in maximum adsorption capacity. The decrease indicates that the formation of water clusters plays a more important role than the better dispersion of MWCNTs for TEX adsorption.

1. Introduction

In the last few decades, one of the most commonly toxic pollutants is the petroleum hydrocarbons due to release of petrol, gasoline, diesel, petrochemical products from storage tanks, wastes from oil industries and improper disposal of hazardous wastes. For many years petroleum hydrocarbons in particular toluene, ethylbenzene and xylene (TEX) have drawn the widespread attention of researchers because groundwater contaminated by TEX is a very serious problem and many communities in the world depend upon groundwater as sole or major source of drinking water. Consequently, sustainable and efficient wastewater treatment for TEX is significantly needed.

Carbon nanotubes (CNTs), a new member of the carbon family, were first rediscovered by Lijima in 1991 [1]. Because of their highly porous and hollow structure, large specific surface areas, surface functional groups and hydrophobic surfaces, CNTs have aroused widespread attention as a new type of adsorbents for the removal of various inorganic and organic pollutants from large volumes of wastewater. The strong adsorption affinity of CNTs towards organic contaminants [2,3], such as TEX [3–7], polyaromatics [8–12], chlorophenols [13–15], 1,2-dichlorobenzene [16], nitrobenzene [11,17], phenolic compounds [18,19], amino acid [20], herbicide [21,22], natural organic matters [23–25], and dyes [26–28] was investigated experimentally or numerically. The adsorption capacity of organic pollutant via CNTs is mainly attributed to the pore structure and the surface oxygen-containing functional groups. Surface functionalization of CNTs is aimed for easy processing, and meanwhile, their adsorption properties with organic chemicals can be altered greatly. The influence of surface oxidation on the adsorption of several typical hydrophobic organic chemicals has been reported [8–10,29,30]. But few studies have discussed the adsorption characters of toluene, ethylbenzene and m-xylene on different oxidized MWCNTs from aqueous solutions. Furthermore, there are the lack of relationships between surface oxidation and adsorption properties. During CNT surface functionalization, purification, or exposure to oxidizing agents after release to the environment, CNTs will eventually be oxidized [10]. Therefore, a better understanding of toxicology and adsorption properties of oxidized CNTs is of importance for CNT environmental risk assessment.

In this paper, MWCNTs are synthesized by the floating catalytic chemical vapor deposition method (CVD) [31], and a highly efficient and nondestructive purified approach has been studied detailed in

* Corresponding author. Tel.: +86 21 34203731; fax: +86 21 54747461.
E-mail address: wuyanqing@sjtu.edu.cn (Y. Wu).

0304-3894/$ – see front matter © 2011 Elsevier B.V. All rights reserved.
doi:10.1016/j.jhazmat.2011.06.048

our previous work [32]. Based on our previous research results, the MWCNTs will be oxidized by NaClO solutions with different concentrations, and then employed as adsorbents to study their physicochemical properties and adsorption characteristics of TEX in aqueous solutions. To eliminate the effects of different oxidants on the adsorption capacity, only the NaClO solutions will be used as the same oxidant to modify the surface of MWCNTs. Adsorption mechanisms will be better understood by investigating the adsorption behaviors of TEX onto MWCNTs with different oxygen contents.

2. Materials and methods

2.1. MWCNTs preparation and purification

The present MWCNTs are prepared by the CVD method [31]. Ethanol is used as carbon feedstock, ferrocene as catalyst, and thiophene as growth promoter. Details on the pristine MWCNTs preparation are given in Supporting Information.

The pristine sample in a quartz boat is put in a quartz tube and heated in air at 400 °C for 45 min to oxidize Fe nanoparticles. Air is introduced into the quartz tube at a slow rate to provide oxygen continuously. After air oxidation, the oxidized sample is further heat-treated at 800 °C or 900 °C for 60 min under the protection of Argon gas, and then refluxed in 3 M HNO_3 for 3 h. The samples after acid treatment are filtered and rinsed with distilled water until the filtrate became neutral.

2.2. Surface modification and characterization of MWCNTs

After the purification treatment, the purified MWCNTs are oxidized by different concentration of NaClO (70% purity). The different concentrations are 30% NaClO (70 mL H_2O + 30 mL NaClO) solution, 15% NaClO (85 mL H_2O + 15 mL NaClO) solution and 3% NaClO (97 mL H_2O + 3 mL NaClO) with magnetic stirring at ambient temperature for 12 h. After oxidation, the mixture is filtered and the filtered solid is washed repeatedly, until the filtrate become neutral. The filtered solid is dehydrated subsequently using vacuum drying oven at 120 °C for 8 h. The purified and oxidized MWCNTs are labeled as CNTs-2.0%O, CNTs-3.2%O, CNTs-5.9%O and CNTs-4.7%O according to their oxygen contents, respectively.

The microstructure and morphology of the purified and oxidized MWCNTs are analyzed by high resolution transmission electron microscopy (HRTEM, JEOL 2100F, accelerating voltage of 200 kV, Japan). The crystal phase of adsorbents is characterized by X-ray diffractometer (XRD, Bruker D8 Advance, Bruker AXS, Germany) using Cu Kα radiation (40 kV and 40 mA). The specific surface area and pore size distribution of adsorbents are calculated from the adsorption–desorption isotherms of N_2 at 77 K by multi-point BET, MP method and BJH method [33,34] using a BELSORP instrument (BEL, Japan, Inc.). Details of N_2 adsorption experiments are given in Supporting Information. The surface functional groups of adsorbents are detected by a Fourier Transform Infrared Ray (FTIR) Spectrometer (NICOLET 5700, America Spectrum One, Perkin Elmer, MA, USA) from 4000 to 400 cm^{-1}. X-Ray photoelectron spectroscopic (XPS) analysis are carried out in a Kratos Axis Ultra DLD Spectrometer, using monochromated Al Ka X-rays, at a base pressure of 1×10^{-9} Torr. The surface chemistry on MWCNTs can have acidic as well as basic properties and can be conveniently determined by titration method [35]. The amount of acidic surface oxygen groups (carboxylic, lactonic, and phenolic groups) is determined using Boehm titration method [35] (Details given in Supporting Information). The number of basic sites is determined from the amount of HCl that reacts with the MWCNTs. TA Instruments® Q600 SDT thermal analyser is used for high resolution thermogravimetric analysis (TGA), differential thermal analysis (DTA) of adsorbents. TGA and DTA curves are obtained by heating approximately 10 mg of finely samples from 40 to 900 °C at a heating rate of 10 °C/min in air atmosphere.

2.3. Batch adsorption experiments

Batch adsorption experiments are conducted in 50 mL headspace bottles equipped with Teflon-lined screw caps with 20 mg MWCNTs and 50 mL TEX solution of different initial concentrations, which result in almost no headspace. The initial concentration of solutions are in the range of 15–110 mg/L for toluene, 10–80 mg/L for ethylbenzene and m-xylene. Sample bottles are shaken on a shaker (TS-2102C, Shanghai, China) and operated at a constant temperature of 20 °C and 180 rpm for 10 h. All the adsorption experiments are conducted at least in duplicate, and only the mean values have been reported. The maximum deviation for the duplicates is usually less than 5%. The blank experiments without the addition of MWCNTs are conducted to ensure that the decrease in the concentration is actually due to the adsorption of MWCNTs, rather than by the adsorption on glass bottle wall or via volatilization. After equilibrium is achieved, the TEX concentration of the supernatant solutions is analyzed by gas chromatograph (GC 2010, Shinmadzu Corporation, Japan) with flame ionization detection (GC-FID) [36]. Kinetic studies are performed with 46, 56 and 47 mg/L initial concentration for toluene, ethylbenzene and m-xylene, respectively. To study the adsorption thermodynamic, the temperature of batch experiment is held at 10, 20 and 45 °C. To study the effects of solution pH on adsorption capacity, batch experiment are conducted in the initial pH range of 2.0–10 with 31, 40 and 32 mg/L initial concentration for TEX, respectively. The initial pH is adjusted using 0.05 M HCl or 0.05 M NaOH solution.

The amount of adsorbed TEX on adsorbents (q_e, mg/g) can be calculated as follows:

$$q_e = (C_0 - C_e) \times \frac{V}{m} \quad (1)$$

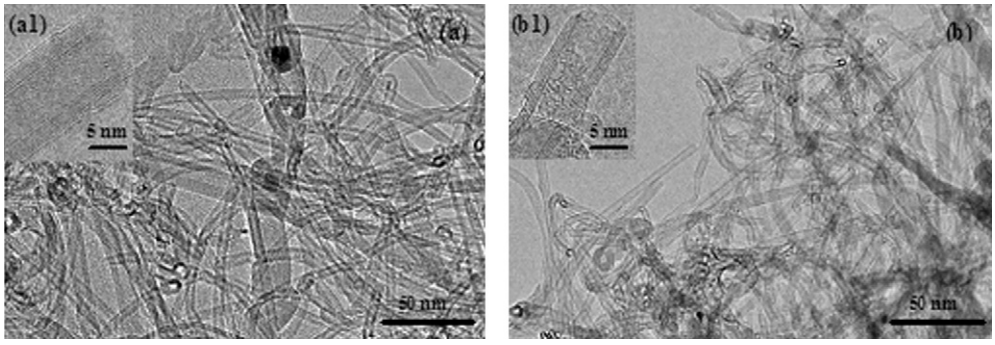

Fig. 1. TEM of CNTs-2.0% O (a,a1) and CNTs-4.7% O (b,b1).

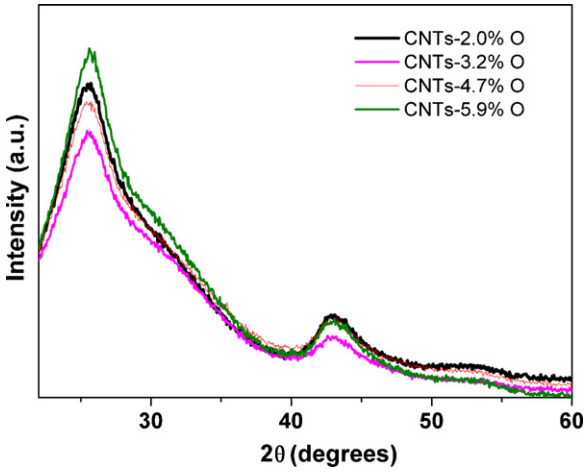

Fig. 2. X-ray diffraction (XRD) patterns of the purified and oxidized MWCNTs.

where C_0 and C_e are the initial and equilibrium TEX concentrations (mg/L),respectively; V is the initial solution volume (L); and m is the adsorbent weight (g).

3. Results and discussion

3.1. Physicochemical characterization of MWCNTs

It is known that oxidants can alter structural and physical properties of MWCNTs [37,38]. The effects of different concentration NaClO solutions were evaluated on structural integrity, surface area and pore distribution.

TEM analysis (see Fig. 1) show that the MWCNTs remain structurally intact after oxidation, which is consistent with Cho' report [10]. The size of outer diameter is less than 10 nm. The TEM images of CNTs-3.2%O and CNTs-5.9%O are similar to that of CNTs-4.7%O and both of their images were not shown in the paper for clarity. The XRD patterns of MWCNTs with different oxygen contents are shown in Fig. 2. These patterns illustrate the characteristics of a typical MWCNT structure, which indicates a typical peak of graphite at $2\theta = 26.1^\circ$ [39]. After the MWCNTs are oxidized, the XRD results clearly demonstrate that the graphitic structures are still preserved in the carbon nanotubes.

The pore size distribution curves of purified and oxidized MWCNTs (see Fig. 3) can be calculated from the adsorption–desorption isotherms of N_2 at 77 K. The physical properties of the purified and oxidized MWCNTs are tabulated in Table 1. The results show that the purified MWCNTs have the greatest ISA, ESA and PV. After oxidation, ISA of all the oxidized MWCNTs are sharply reduced, ESA and PV of those are reduced, and APD slightly increased. Similar results have been reported in the literature [7]. Comparing CNTs-3.2%O with CNTs-4.7%O, they have similar variation trend with SSA, ISA, ESA, PV and APD, which show that they have the same physical properties according to Table 1 and Fig. 3. More interestingly,

Table 1
Physicochemical properties of the purified and oxidized MWCNTs.

Sorbent	SSA	ISA	ESA	PV	APD	O%	O%-$_{SSA}$
CNTs-2.0%O	471	136	335	0.64	5.4	2.0	4.25
CNTs-3.2%O	381	61	320	0.58	6.0	3.2	8.40
CNTs-4.7%O	382	74	308	0.58	6.0	4.7	12.30
CNTs-5.9%O	327	50	277	0.49	5.9	5.9	18.04

Note: SSA = special surface area (m^2/g); ISA = internal surface area (m^2/g); ESA = external surface area (m^2/g); PV = pore volume (cm^3/g); APD = average pore diameter (nm); O%: surface oxide (at. %) by XPS; O%-$_{SSA}$ means that special surface area normalized surface oxides values.

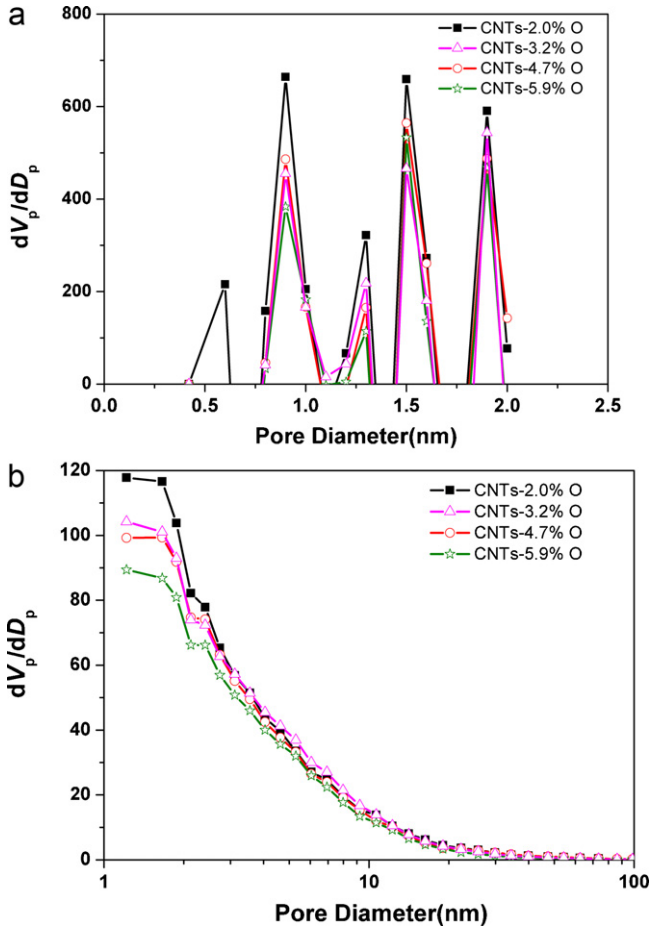

Fig. 3. Micropore distributions (a) and mesopore distribution (b) of the purified and oxidized MWCNTs.

the SSA of CNTs-5.9%O has decreased greatly than CNTs-3.2%O and CNTs-4.7%O. 15% NaClO has stronger oxidability than 3% NaClO, and more micropores could be enlarged into mesopores or more mesopores are destroyed. Consequently, SSA decrease. With the increasing of oxidability for 30% NaOCl, some new pores may be produced or two tips of some MWCNTs may be opened, and thus the total surface area will significantly increase compared with 15% NaOCl.

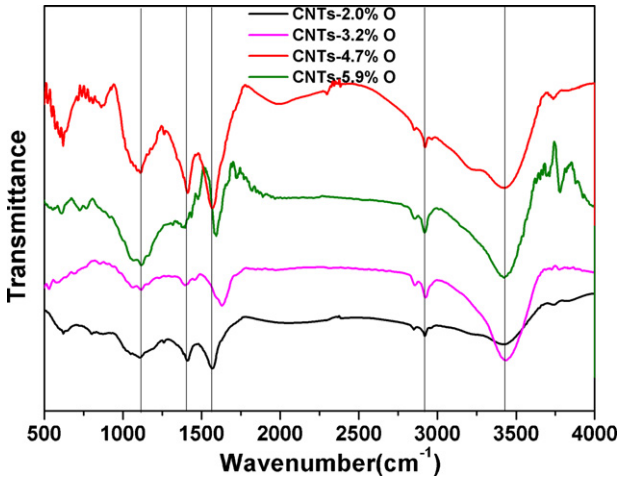

Fig. 4. FTIR spectra of the purified and oxidized MWCNTs.

The FTIR spectra (see Fig. 4) confirmed the existence of some significantly apparent bands of the purified and the treated MWCNTs. It is clear that the sharp peak at 3430 (1/cm) are assigned to –OH stretch from carboxylic groups (–COOH and –COH) [40]. The bands at 1580 and 1405 (1/cm) are C=O groups [41] and carboxylate anion stretch mode [40]. The band at ~1112 (1/cm) is associated to C–O stretching of alcoholic compounds [42]. These functional groups existed in the external and internal surface become stronger after oxidation, which increase the surface polarity and further alter the surface charges properties. For example, after oxidation, the zeta potentials of CNTs-2.0%O is obviously reduced from −24.9 mV to −33.7 mV, −33.0 mV and −30.8 mV for CNTs-3.2%O, CNTs-4.7%O and CNTs-5.9%O, respectively, when the solution pH is near neutral.

With reference to functionality grafting, XPS is one of the surface analytical techniques, which can provide useful information on the nature of the functional groups and also on the presence of structural defects on the nanotube surface. The wide scan XPS spectra of purified and oxidized MWCNTs are shown in Fig. 5a. The XPS O1s peaks (see Fig. 5b) of the MWCNTs confirmed the presence of some oxygen-containing functional groups onto the MWCNTs surface. The surface oxygen content on the MWCNTs detected by XPS measurements for each treatment is given in Table 1. As is an evident, there is a clear increase of oxygen content on the walls of MWCNTs for all treatments attempted here. The total surface oxygen amounts on the purified and oxidized MWCNTs are 2.0, 3.2, 4.7, and 5.9 at. %, respectively. Deconvolution of the C1s peak (see Fig. 5c–f) of the purified and oxidized MWCNTs show a main peak of sp^2 C=C (284.38–284.53 eV) attribute to the graphitic structure. Moreover, a peak of sp^3 C–C (285.11–285.5 eV) is attributed to defects on the nanotube structure. Peaks at 286.21–287.53 eV, 286.45–287.92 eV, and 288.39–289.54 eV correspond to carbon atoms attached to different oxygen-containing moieties.

The results of Boehm titration are given in Table 2. It is clear that the number of oxygenated acidic functional groups increases with the increasing of oxygen content, which could be caused by the presence of more carboxyls, phenols or lactones on the MWCNT

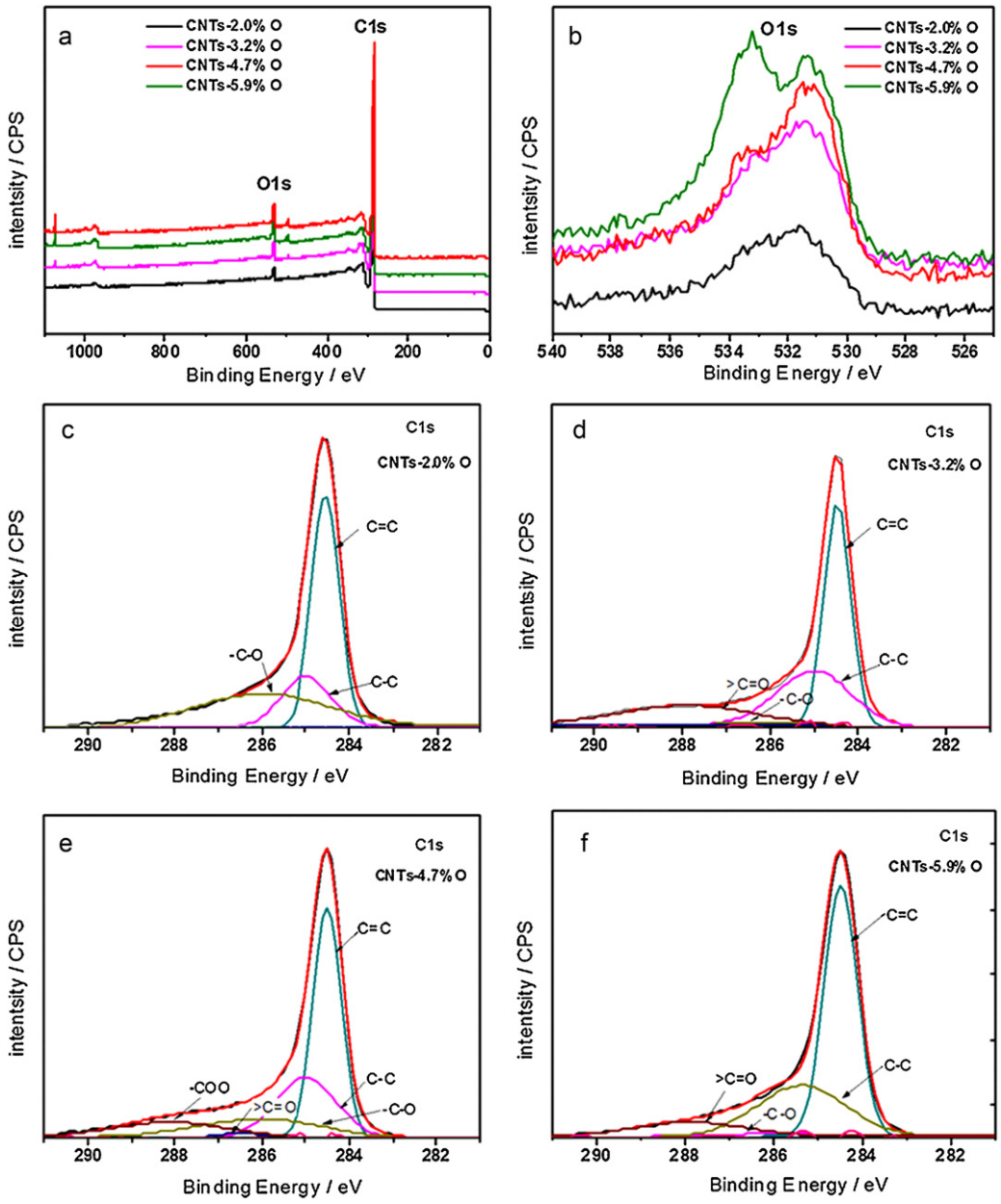

Fig. 5. XPS spectra of adsorbents: XPS wide-scan (a), O1s (b), and C1s high-resolution spectra of CNTs–2.0%O (c), CNTs–3.2%O (d), CNTs–4.7%O(e), and CNTs–5.9%O (f).

Table 2
Surface chemistry of the purified and oxidized MWCNTs.

Adsorbents	Carboxylic groups (mmol/g)	Lactonic groups (mmol/g)	Phenolic group (mmol/g)	Total acidity (mmol/g)	Total basicity (mmol/g)
CNTs-2.0%O	0.0025	0.023	0.016	0.042	0.106
CNTs-3.2%O	0.0054	0.021	0.045	0.072	0.138
CNTs-4.7%O	0.0047	0.014	0.111	0.129	0.111
CNTs-5.9%O	0.0005	0.029	0.267	0.297	0.16

wall and may provide more active sites for facilitating TEX adsorption. Phenolic groups predominate after oxidation as their number increase from 62% to 90% of total acidity with the increasing from 3.2% to 5.9% of oxygen content. Acidic and bacis surface sites coexist usually. The total basicity of MWCNTs also increased after the oxidation, which may be caused by the presence of more oxygen functional groups and the existence of pyrone-type structures on the edges of the polyaromaticlayers [35]. However, the origin of surface basicity after oxidation of MWCNTs is still under discussion. The result is not in accord with some previous researches that the basiticy values decrease with the increase in the amount of acidic surface groups [35,43]. Therefore, further studies are needed for elucidating surface oxygen functional groups effects on TEX adsorption.

It is well known that different structural forms of carbon can exhibit different oxidation behaviors depending each time on the available reactive sites [44,45]. Thermo gravimetric curves (TG) and differential thermal analytic curves (DTA) have been widely utilized to make qualitative and quantitative studies of the oxidative behaviors for various sorbents (see Fig. 6). In Fig. 6a, all the TG curves of MWCNTs exhibit three main weight loss regions. All of the MWCNTs are considerably stable and show a little weight loss close to 5% below 200 °C in the first region, which can be attributed to the evaporation of adsorbed water and the elimination of carboxylic groups and hydroxyl groups on the MWCNT wall [46]. The rapid weight loss region can be due to the decomposition of carbon in the MWCNTs. The third region displays a little weight loss close, in which 8.4%, 1.7%, 4.7%, and 3.9% remaining weight are observed at 900 °C for CNTs-2.0%O, CNTs-3.2%O, CNTs-4.7%O, CNTs-5.9%O, respectively. The temperatures at which the main thermal events took place during the whole oxidation process may be identified from the DTA curves (see Fig. 6b). While for the purified MWCNTs samples, the events might occur at temperatures from 500 °C to 625 °C, the main thermal oxidation took place at ~600 °C, but for oxidized MWCNTs samples having undergone lower temperature treatment. Comparing CNTs-3.2%O sample with CNTs-2.0%O, it is clearly seen that the main thermal events temperature (Tm) is decreased from 600 °C to 550 °C, which may be attributed to the MWCNTs structure destroyed by oxidants. Comparing the purified MWCNTs with oxidized MWCNTs, the trend of Tm indicates that the oxygen content strongly affects the thermal-oxidative stability of MWCNTs. The higher oxygen content is, the lower the thermal-oxidative stability of MWCNTs is. There is an indication that the CNTs-3.2%O is more oxidation-resistant than CNTs-4.7%O, CNTs-5.9%O.

3.2. TEX adsorption isotherms and comparison of contaminants adsorption characters

The adsorption equilibrium data of TEX on the purified and oxidized MWCNTs are fitted by several well-known isotherm models to assess their efficacies. The adsorption isotherms are presented in Fig. 7. All isotherms exhibited non-linear and are described with Langmuir model and Freundlich model, which can be expressed respectively as:

$$q_e = \frac{q_m K_l C_e}{1 + K_l C_e} \quad (2)$$

$$q_e = K_f C_e^n \quad (3)$$

where C_e and q_e is the concentration of contaminants in water and adsorbent when the adsorption equilibrium reaches, respectively; q_m is the maximum adsorption capacity; K_l is the adsorption equilibrium constant of Langmuir model; K_f and n (typically < 1) are Freundlich constants related to adsorption capacity and adsorption intensity of the adsorbents, respectively. The regression data for all materials of two models are tabulated in Table 3. The coefficients of determination R^2 in Langmuir model is higher than those of Freundlich model for TEX. Therefore, Langmuir model is more suitable to simulate the TEX adsorption isotherms.

At any given value of C_e (see Fig. 7), it is an evident that the adsorption capacity of TEX on CNTs-3.2%O is larger than those of other materials. The maximum adsorption capacities calculated by Langmuir model (see Table 3) for TEX are generally in accordance with the order: CNTs-3.2%O > CNTs-4.7%O > CNTs-2.0%O > CNTs-5.9%O. Based on results at the highest C_e of TEX, q_m is approximately 3 times higher for CNTs-3.2%O than for CNTs-

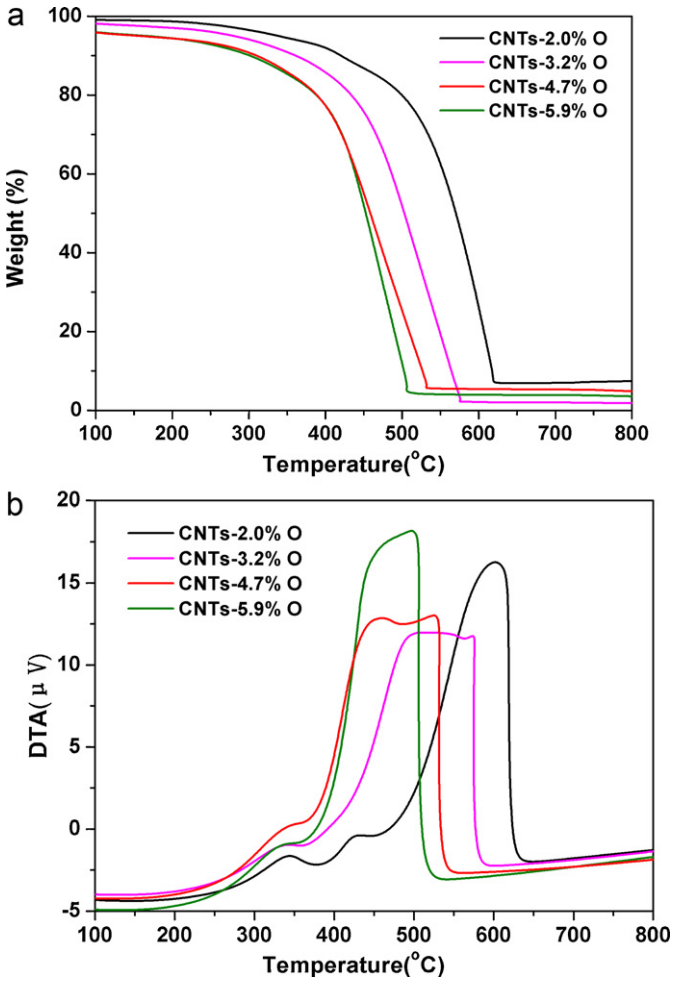

Fig. 6. TG(a) and DTA(b) of the purified and oxidized MWCNTs.

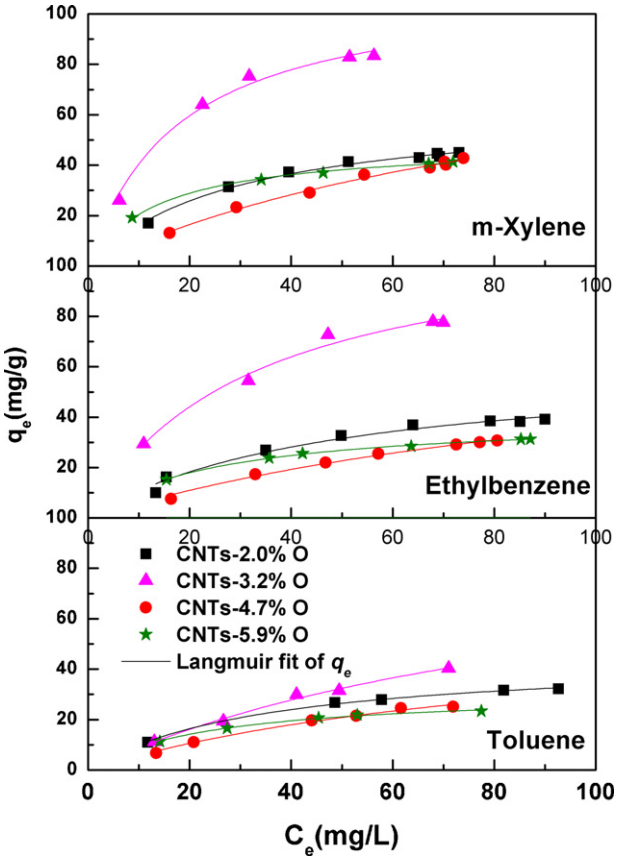

Fig. 7. Adsorption isotherms of TEX on the purified and oxidized MWCNTs under pH 7. Lines through the data are based on fits obtained using the Langmuir adsorption model.

5.9%O and almost 2 times than for CNTs-2.0%O. The maximum adsorption capacity of CNTs-3.2%O, CNTs-4.7%O, CNTs-2.0%O, and CNTs-5.9%O, respectively, are 99.47, 59.48, 44.90 and 31.28 mg/g for T; 115.63, 79.15, 61.12, and 40.18 mg/g for E; 112.19, 100.45, 62.82 and 48.73 mg/g for m-X.

For different adsorbents, q_e values follow the orders (see Fig.S1): m-X > E > T with different initial concentration of TEX. From Table 3 view, q_m values follow the orders: m-X > E > T for CNTs-2.0%O, CNT-4.7%O and CNT-5.9%O with different initial concentration TEX, and E > m-X > T for CNT-3.2%O. Favorable adsorption of those order of contaminants may be attributed to the decrease in solubility (T, 515 mg/L > m-X, 175 mg/L > E, 152 mg/L), and the increase in molecular weight (T, 92.15 < E, X, 106.18) and boiling point (T, 110.63 °C < E, 136.19 °C < m-X, 139.1 °C). Nonetheless, it is not completely consistent with physical property of adsorbates.

3.3. Adsorption kinetics

Adsorption kinetic is one of the most important characters which govern the solute uptake rate and represents the adsorption efficiency of the adsorbent and therefore, determines its potential applications. The adsorption kinetics experiments of TEX on CNTs-3.2%O are conducted under pH 7. As shown in Fig. 8a, fast initial adsorption from liquid to the CNTs-3.2%O is obviously observed within 60 min for TEX, which suggests a rapid initial transfer of TEX into the near surface boundary layers of CNTs-3.2%O. At this stage, this maximum is a little larger than the equilibrium adsorbed amount. When the solution begins to interact with the solid, the large difference in solute concentration between phases causes rapid movement of solute. Large numbers of pores in the correct size range assist with pore-filling and capillary condensation [47], so the solute "sorbed" in the solid becomes larger until a maximum is reached; such solute distribution is only a transient phenomenon, not true adsorption equilibrium. In the next stage, the new equilibrium distribution begins with diffusion of "sorbed" solute from solid to solution [48]. The kinetic curve shows that the "sorbed" amount decreases with time till the values have a stable value. This progress is followed by a slow diffusion from externals sites to internal sites of CNTs-3.2%O. Finally, the adsorption reaches equilibrium gradually within 6 h for TEX.

To further understand the adsorption kinetics, the pseudo-second-order model is selected to fit the kinetic data, which is depicted by Eq. (4) [49]:

$$\frac{t}{q_t} = \frac{1}{k_2 q_e^2} + \frac{1}{q_e} t \tag{4}$$

where q_e and q_t are the concentrations of TEX adsorbed on CNTs-3.2%O at equilibrium and at various time t, respectively; k_2 is the rate constant of Eq. (4) for adsorption. Furthermore, the slope and intercept of the linear plot of t/q_t against t yielded the values of $1/q_e$ and $1/k_2 q_e^2$ for Eq. (4).

The linear regression of adsorption kinetics is shown in Fig. 8b and the related model parameters are listed in Table 4. It is found that the pseudo-second-order model fitted all the adsorption data well with correlation coefficient (R^2) up to 0.986–0.997 for TEX, indicating that the chemical interactions are possibly involved in the adsorption processes and the adsorption capacity is proportional to the number of active sites on CNTs-3.2%O [50,51].

Table 3
Parameters of the Langmuir and the Fruendlich models for adsorption of TEX on the purified and oxidized MWCNTs.

Adsorbate	Adsorbents	Langmuir constants			Fruendlich constants		
		q_m (mg/g)	K_l (L/mg)	R^2	K_f (mg/g)	n	R^2
Toluene							
	CNTs-3.2%O	99.47	0.010	0.99	1.87	0.726	0.98
	CNTs-4.7%O	59.48	0.011	0.99	1.22	0.721	0.98
	CNTs-5.9%O	31.28	0.041	0.99	4.28	0.401	0.94
Ethylbenzene	CNTs-2.0%O	61.12	0.021	0.97	3.64	0.539	0.94
	CNTs-3.2%O	115.63	0.031	0.98	9.92	0.493	0.95
	CNTs-4.7%O	79.15	0.008	0.99	1.23	0.739	0.98
	CNTs-5.9%O	40.18	0.040	0.99	6.04	0.372	0.96
m-Xylene	CNTs-2.0%O	62.82	0.035	0.99	6.69	0.449	0.95
	CNTs-3.2%O	112.19	0.057	0.99	15.09	0.437	0.91
	CNTs-4.7%O	100.45	0.010	0.99	2.04	0.706	0.98
	CNTs-5.9%O	48.73	0.073	0.99	9.69	0.344	0.98

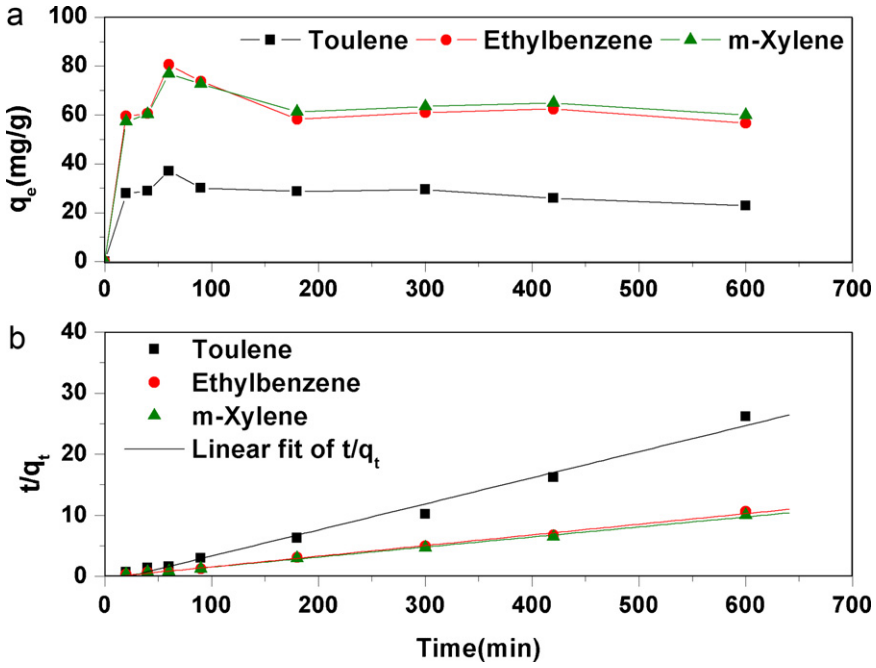

Fig. 8. (a) Adsorption kinetics of TEX on CNTs-3.2%O under pH 7. (b) Linear regression of kinetics plots. Lines through the data are based on fits obtained using the pseudo-second-order model.

3.4. Thermodynamic analysis

The thermodynamic parameters provide in-depth information on inherent energetic changes that are associated with adsorption; therefore, they should be properly evaluated. To determine the effect of temperature on TEX adsorption, adsorption experiments were also conducted at 10, 20 and 45 °C. The effect of temperature on the sorption of TEX is shown in Fig. 9. An increase in temperature resulted in a corresponding decrease in the adsorption of TEX. This observation indicates that the uptake of TEX on CNTs-3.2%O is an exothermic process. The thermodynamic parameters such as change in Gibbs free energy (ΔG°), enthalpy (ΔH°), and entropy (ΔS°) are calculated by using the following equations:

$$\Delta G^\circ = -RT \ln K_0 \quad (5)$$

$$\Delta S^\circ = \frac{\Delta H^\circ - \Delta G^\circ}{T} \quad (6)$$

where K_0 is the thermodynamic equilibrium constant. As the TEX concentration in the solution decreases and approaches to 0, values of K_0 are obtained by plotting a straight line of $\ln(q_e/C_e)$ versus q_e based on a least-square analysis and extrapolating q_e to 0. Subsequently, the intercept of vertical axis gives the value of $\ln K_0$. The ΔH° is determined from the slope of the regression line after plotting $\ln K_0$ against the reciprocal of absolute temperature, $1/T$. The ΔG° and ΔS° are determined from Eqs. (5) and (6), respectively.

The thermodynamic parameters are listed in Table 5. The negative ΔH° indicates the exothermic nature of adsorption process for TEX on CNTs-3.2%O, which is supported by the decrease of TEX adsorption onto CNTs-3.2%O with a rise in temperature, as shown in Fig. 9. The ΔG° values were negative for TEX at all three temperatures, which implies that the adsorption of TEX by CNTs-3.2%O was spontaneous and thermodynamically favorable. Furthermore, a more negative ΔG° implies a greater driving force of adsorption,

Table 4
Kinetics parameters of the pseudo-second-order model for TEX on CNTs-3.2%O under pH 7.

Adsorbate	C_0 (mg/L)	$q_{e,exp}$ (mg/g)	Pseudo-second order parameter		
			K_2 g/(mg h)	$q_{e,cal}$ (mg/g)	R^2
T	46.2	22.93	0.116	23.42	0.986
E	56.8	58.28	0.095	57.47	0.995
M-X	47.2	61.34	0.134	60.98	0.997

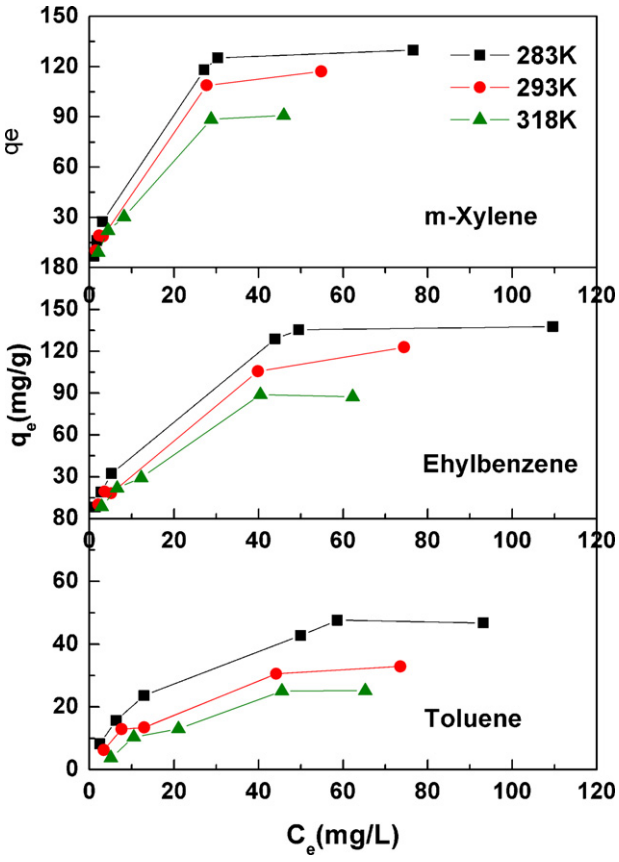

Fig. 9. Adsorption isotherms of TEX on CNTs-3.2%O at various temperatures.

Table 5
Thermodynamic parameters on the adsorption of TEX by CNTs-3.2%O under pH 7.

	Temperature (K)	$\ln K_0$	ΔG° (kJ/mol)	ΔH° (kJ/mol)	ΔS° (kJ/mol)
Toluene	283	1.57	−3.69		−70.49
	293	1.06	−2.59	−23.64	−71.84
	318	0.43	−1.13		−70.78
Ethylbenzene	283	2.02	−4.76		−43.59
	293	1.66	−4.04	−17.10	−44.59
	318	1.20	−3.17		−43.82
m-Xylene	283	1.89	−4.45		−27.25
	293	1.69	−4.12	−12.91	−26.66
	318	1.36	−3.61		−27.12

resulting in a higher adsorption capacity (see Fig. 9 and Table 5). The negative ΔS° indicated the decrease in randomness at the solid/liquid interface during adsorption of TEX on CNTs-3.2%O.

3.5. Influence of MWCNTs with surface oxygen contents on TEX adsorption

From Fig. 7 view, it is evident that q_e is significantly enhanced with the CNTs-3.2%O, but is dramatically reduced with the CNTs-5.9%O. And the order of equilibrium adsorption amounts (q_m) of TEX from the greatest is CNTs-3.2%O, CNTs-4.7%O, CNTs-2.0%O, and CNTs-5.9%O. From Table 1 view, the trend of q_m is not significantly consistent with the changes of surface area, pore diameter or pore volume, but is greatly in agreement with the surface oxygen contents of MWCNTs. This suggests that changes in equilibrium sorption capacity upon oxidation are principally caused by changes in surface chemistry, notably surface oxygen content. Since the surface area is one of factors influencing the adsorption capacity, surface oxygen contents of MWCNTs are normalized by SSA (see Table 1) to analysis the influence of MWCNTs with different surface oxygen contents on TEX adsorption. This is well described in terms of the maximum adsorption volume (q_m) from Langmuir adsorption model, as shown in Fig. 10. The results in Fig. 10 and Table 1 reveal that a 4.15% increase in oxygen concentration from 4.25% to 8.4% leads to a 122%, 89%, 79% increase in maximum sorption capacity for TEX adsorption, a 8.05% increase from 4.25% to 12.3% leads to a 32%, 29%, 60% increase for TEX adsorption, but more interestingly, a 13.79% increase from 4.25% to 18.04% leads to a 30%, 34%, 22% decrease for TEX adsorption, respectively. Moreover, when the oxygen contents of MWCNTs are roughly higher than 15.27%, 14.95%, 16.48% for TEX, maximum adsorption capacity will begin to lower compared with the MWCNTs with 2.0% oxygen content on a linear assumption for the changes (see Fig. 10).

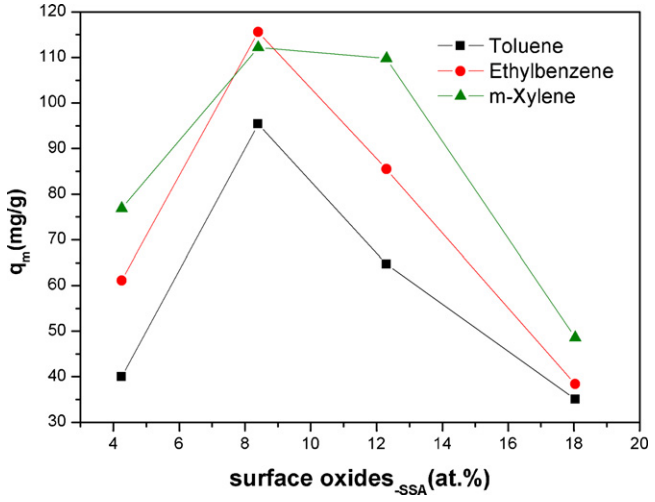

Fig. 10. Maximum adsorption capacity (q_m) for TEX from the Langmuir adsorption model plotted against surface oxygen concentration.

Although maximum adsorption capacities strongly correlate with the extent of surface oxidation, the results clearly show that it is not a systematic increase or decrease in the extent of TEX maximum adsorption with increasing level of oxidation. Here, surface oxygen content affects two sides, the dispersibility and water cluster formation, which consequently can be favorable or unfavorable for the aqueous phase adsorption. With the increasing of oxygen content, from 4.25% to 8.4%, maximum adsorption capacity is significantly enhanced. Similar results have been reported for BTEX adsorption on MWCNTs [6,7]. The results of Boehm titration indicated that total acidity functional groups increases with the increasing of oxygen contents. In this stage, the main purpose of the surface functionalization of the MWCNTs is to improve their hydrophilicity and dispersibility in aqueous solutions. A better dispersion (see Fig.S2) of the MWCNTs in water increases the available adsorption sites, which consequently can be favorable for the aqueous phase adsorption. Therefore, the dispersive interactions are predominant. TEX are in the molecular form in the whole ranges of pH, and thus, the adsorption mechanism of TEX via MWCNTs is mainly attributed to the π–π electron-donor–acceptor interaction between the electronic density in the TEX aromatic rings and the π orbital on the MWCNTs [52,53]. At the second stage, when the surface oxygen concentration increases to a certain extent, for example, from 8.4% to 12.3%, MWCNTs lead to lower TEX adsorption capacity than that of CNTs-3.2%O, but still higher than that of CNTs-2.0%O. Although their dispersion is also improved by surface functionalization in aqueous solutions, it remarkably decreases the maximum adsorption capacities of TEX due to water cluster formation caused by introduced phenolic groups on the surface or tube end of MWCNTs through hydrogen bonding at hydrophilic sites, which is in agreement with Wang's report [54]. Here, their dispersion plays a more important role than the water cluster formation, and thus, the adsorption is considerably higher than that of CNTs-2.0%O. When oxygen concentration goes on increasing, for example, from 12.3% to 18.04%, MWCNTs significantly decrease in maximum adsorption capacity, and even lower than CNTs-2.0%O. In this process with the increasing of oxygen concentration and phenolic groups, the overall decrease in the adsorption of TEX indicates that water cluster formation plays a more important role in the adsorption of TEX than the better dispersion of MWCNTs in water, and thus, the maximum adsorption of TEX on CNTs-5.9%O is less than on CNTs-2.0%O. The decrease in adsorption after oxidation of CNTs has also been observed for polyaromatics in previous studies [8,10,30,43].

Furthermore, TEX adsorption capacity is in agreement with the order of carboxylic groups though these concentrations are relative low (CNTs-3.2%O > CNTs-4.7%O > CNTs-2.0%O > CNTs-5.9%O), which indicated carboxyls groups may play a key role in TEX adsorption. And the electrostatic interaction between the TEX

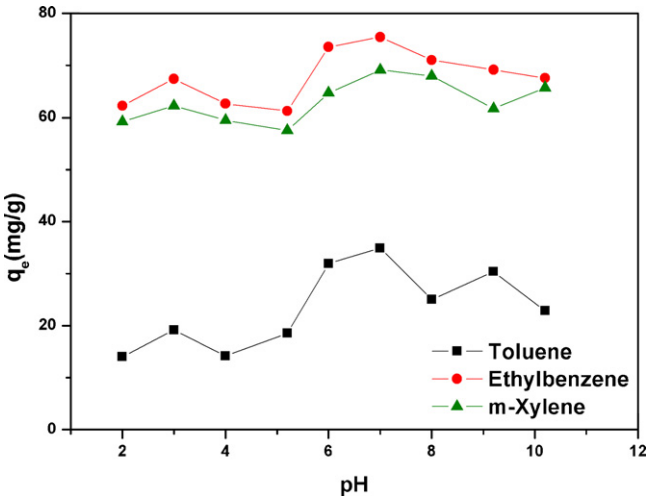

Fig. 11. Effect of initial pH on TEX adsorption on CNTs-3.2%O.

molecules and the MWCNTs surface may also explain the observation of high TEX adsorption via the purified MWCNTs and oxidized MWCNTs. Since the TEX molecules are positively charged, which have been reported in the literature for TEX adsorption on MWCNTs, adsorption of TEX is thus favored for adsorbents with a negative surface charge [2,7,18]. The zeta potentials of the CNTs-3.2%O and CNTs-4.7%O at a pH of 7 are −33.7 and −33.0 mV, which also leads to a high TEX adsorption for the electrostatic attraction [8,10,30].

3.6. Effect of initial pH on adsorption

To gain further insight into the adsorption process, the effect of initial pH on the adsorption of TEX by CNTs-3.2%O is studied and the results are presented in Fig. 11. It is observed that three adsorbates have the similar changes with the effect of initial pH. With increasing pH values, the adsorption capacity for TEX first slightly decreases and then increases, finally a little decreases again. TEX has the maximum value of the adsorption capacity under pH 7. Overall, the adsorption of TEX on CNTs-3.2%O is not greatly sensitive with initial pH variation of the solution, reflecting high stability of CNTs-3.2%O as TEX adsorbents in wide range of solution pH, which is consistent with the previous research [5,6].

4. Conclusion

MWCNTs are fabricated by CVD methods and oxidized by different concentration NaClO solutions to avoid the effects of different oxides. The purified and oxidized MWCNTs are employed as adsorbents to study their physicochemical properties and adsorption performance of three priority pollutants namely TEX in an aqueous solution. The results indicate that the q_e is significantly enhanced with CNTs-3.2%O and CNTs-4.7%O, but is markedly reduced by CNTs-5.9%O. Langmuir model is more suitable to simulate the TEX adsorption isotherms than Freundlich model. The adsorption kinetics for TEX onto CNTs-3.2%O is well accurately represented by the pseudo second-order model. Thermodynamic study shows endothermic, entropy favorable and spontaneous adsorption behavior of TEX by CNTs-3.2%O. The maximum adsorption capacity (q_m) of TEX is approximately 3 times higher for CNTs-3.2%O than for CNTs-5.9%O and almost 2 times than for CNTs-2.0%O. The trend of q_m is strongly correlation with the extent of surface oxygen contents of MWCNTs. This suggests that changes in equilibrium adsorption capacity upon oxidation are principally caused by changes in surface chemistry, notably surface oxygen content. With increasing level of oxidation, the maximum adsorption capacities for TEX divide into two stages. At the first stage, maximum adsorption capacity is significantly enhanced with the increasing of oxygen content. The surface functionalization of the MWCNTs can improve their dispersibilities in aqueous solutions. A better dispersion in water will increase the available adsorption sites, and thus, the dispersive interactions are predominant. At the second stage, when the surface oxygen concentration increases to a certain extent, MWCNTs lead to lower maximum adsorption capacity for TEX. Surface functionalization remarkably decreases the TEX adsorption due to water cluster formation caused by oxygen-containing functional groups on the surface or tube end of MWCNTs. The overall decrease in the adsorption of TEX indicates that water cluster formation played a more important role in the TEX adsorption than the better dispersion of MWCNTs in water. Consequently, the proper control of oxygen content would be beneficial to maximize the absorption capacity of MWCNTs. Furthermore, the electrostatic interaction is one of the adsorption mechanisms of TEX via MWCNTs. The adsorption capacities of TEX on CNTs-3.2%O appear no significant changes with solution pH, reflecting good stability of CNTs-3.2%O as TEX adsorbents in wide range of solution pH. The results highlight the important role of surface oxygen contents in controlling the adsorption properties of TEX onto MWCNTs in wastewater treatment.

Acknowledgments

This research was supported by the National High Technology Research and Development Program of China (863 Program, Grant No.2007AA06Z334) and supported by the Shanghai Jiao Tong University Innovation Fund for Postgraduates. We are also thankful to the reviewers for their valuable comments to improve this manuscript.

Appendix A. Supplementary data

Supplementary data associated with this article can be found, in the online version, at doi:10.1016/j.jhazmat.2011.06.048.

References

[1] S. Lijima, Helical microtubules of graphitic carbon, Nature 354 (1991) 56–58.
[2] B. Pan, B.S. Xing, Adsorption mechanisms of organic chemicals on carbon nanotubes, Environ. Sci. Technol. 42 (2008) 9005–9013.
[3] W. Chen, L. Duan, D.Q. Zhu, Adsorption of polar and nonpolar organic chemicals to carbon nanotubes, Environ. Sci. Technol. 41 (2007) 8295–8300.
[4] L.M. Woods, Ş.C. Bădescu, T.L. Reinecke, Adsorption of simple benzene derivatives on carbon nanotubes, Phys. Rev. B 75 (2007) 155415.
[5] C.J.M. Chin, L.C. Shih, H.J. Tsai, T.K. Liu, Adsorption of o-xylene and p-xylene from water by SWCNTs, Carbon 45 (2007) 1254–1260.
[6] F.S. Su, C.S. Lu, S.K. Hu, Adsorption of benzene, toluene, ethylbenzene and p-xylene by NaOCl-oxidized carbon nanotubes, Colloid Surface A 353 (2010) 83–91.
[7] C. Lu, F.S. Su, S.K. Hu, Surface modification of carbon nanotubes for enhancing BTEX adsorption from aqueous solutions, Appl. Surf. Sci. 254 (2008) 7035–7041.
[8] S.J. Zhang, T. Shao, S.S.K. Bekaroglu, T.J. Karanfil, The impacts of aggregation and surface chemistry of carbon nanotubes on the adsorption of synthetic organic compounds, Environ. Sci. Technol. 43 (2009) 5719–5725.
[9] S. Gotovac, C.M. Yang, Y. Hattori, K. Takahashi, H. Kanoh, K. Kaneko, Adsorption of polyaromatic hydrocarbons on single wall carbon nanotubes of different functionalities and diameters, J. Colloid Interface Sci. 314 (2007) 18–24.
[10] H.H. Cho, B.A. Smith, J.D. Wnuk, D.H. Fairbrother, W.P. Ball, Influence of surface oxides on the adsorption of naphthalene onto multiwalled carbon nanotubes, Environ. Sci. Technol. 42 (2008) 2899–2905.
[11] J. Chen, W. Chen, D.Q. Zhu, Adsorption of nonionic aromatic compounds to single-walled carbon nanotubes: effects of aqueous solution chemistry, Environ. Sci. Technol. 42 (2008) 7225–7230.
[12] S. Gotovac, H. Honda, Y. Hattori, K. Takahashi, H. Kanoh, K. Kaneko, Effect of nanoscale curvature of single-walled carbon nanotubes on adsorption of polycyclic aromatic hydrocarbons, Nano Lett. 7 (2007) 583–587.
[13] Q. Liao, J. Sun, G. Lian, Adsorption of chlorophenols by multi-walled carbon nanotubes treated with HNO_3 and NH_3, Carbon 46 (2008) 553–555.

[14] M.A. Salam, R.C. Burk, Thermodynamics of pentachlorophenol adsorption from aqueous solutions by oxidized multi-walled carbon nanotubes, Appl. Surf. Sci. 255 (2008) 1975–1981.
[15] G.C. Chen, X.Q. Shan, Y.S. Wang, B. Wen, Z.G. Pei, Y.N. Xie, T. Liu, J.J. Pignatello, Adsorption of 2,4,6-trichlorophenol onto multi-walled carbon nanotubes as affected by Cu (II), Water Res. 43 (2009) 2409–2418.
[16] X. Peng, Y. Li, Z. Luan, Z. Di, H. Wang, B. Tian, Z. Jia, Adsorption of 1,2-dichlorobenzene from water to carbon nanotubes, Chem. Phys. Lett. 376 (2003) 154–158.
[17] X.E. Shen, X.Q. Shan, D.M. Dong, X.Y. Hua, G. Owens, Kinetics and thermodynamics of sorption of nitroaromatic compounds to as-grown and oxidized multiwalled carbon nanotubes, J. Colloid Interface Sci 330 (2009) 1–8.
[18] D. Lin, B. Xing, Adsorption of phenolic compounds by carbon nanotubes: role of aromaticity and substitution of hydroxyl groups, Environ. Sci. Technol. 42 (2008) 7254–7259.
[19] G.D. Sheng, D.D. Shao, X.M. Ren, X.Q. Wang, J.X. Li, Y.X. Chen, X.K. Wang, Kinetics and thermodynamics of adsorption of ionizable aromatic compounds from aqueous solutions by as-prepared and oxidized multiwalled carbon nanotubes, J. Hazard. Mater. 178 (2010) 505–516.
[20] J. Zhong, J. Meng, X. Liang, L. Song, T. Zhao, S. Xie, K. Ibrahim, H. Qian, J. Wang, J. Guo, H. Xu, Z. Wu, XANES study of phenylalanine and glycine adsorption on single-walled carbon nanotubes, Mater. Lett. 63 (2009) 431–433.
[21] G.C. Chen, X.Q. Shan, Y.Q. Zhou, X.E. Shen, H.L. Hang, S.U. Khan, Adsorption kinetics, isotherms and thermodynamics of atrazine on surface oxidized multiwalled carbon nanotubes, J. Hazard. Mater. 169 (2009) 912–918.
[22] G.C. Chen, X.Q. Shan, Y.S. Wang, Z.G. Pei, X.E. Shen, B. Wen, G. Owens, Effects of copper, lead, and cadmium on the sorption and desorption of atrazine onto and from carbon nanotubes, Environ. Sci. Technol. 42 (2008) 8297–8302.
[23] K. Yang, B. Xing, Adsorption of fulvic acid by carbon nanotubes from water, Environ. Pollut. 157 (2009) 1095–1100.
[24] X. Wang, S. Tao, B. Xing, Sorption and competition of aromatic compounds and humic acid on multiwalled carbon nanotubes, Environ. Sci. Technol. 43 (2009) 6214–6219.
[25] C. Lu, F. Su, Adsorption of natural organic matter by carbon nanotubes, Sep. Purif. Technol. 58 (2007) 113–121.
[26] C.Y. Kuo, C.H. Wu, J.Y. Wu, Adsorption of direct dyes from aqueous solutions by carbon nanotubes: determination of equilibrium, kinetic and thermodynamics parameters, J. Colloid Interface Sci. 327 (2008) 308–315.
[27] C.H. Wu, Adsorption of reactive dye onto carbon nanotubes: equilibrium, kinetics and thermodynamics, J. Hazard. Mater. 144 (2007) 93–100.
[28] A.K. Mishraa, T. Arockiadossa, S. Ramaprabhu, Study of removal of azo dye by functionalized multi walled carbon nanotubes, Chem. Eng. J. 162 (2010) 1026–1034.
[29] B. Smith, K.E. Schrote, H.H. Cho, W.P. Ball, D.H. Fairbrother, Influence of surface oxides on the colloidal stability of multi-walled carbon nanotubes: a structure–property relationship, Langmuir 25 (2009) 9767–9776.
[30] X.N. Li, H.M. Zhao, X. Quan, S. Chen, Y.B. Zhang, H.T. Yu, Adsorption of ionizable organic contaminants on multi-walled carbon nanotubes with different oxygen contents, J. Hazard. Mater. 186 (2011) 407–415.
[31] J. Ma, J.N. Wang, X.X. Wang, Large-diameter and water-dispersible single-walled carbon nanotubes synthesis, characterization and applications, J. Mater. Chem. 19 (2009) 3033–3041.
[32] J. Ma, J.N. Wang, Purification of single-walled carbon nanotubes by a highly efficient and nondestructive approach, Chem. Mat. 20 (2008) 2895–2902.
[33] S.J. Gregg, K.S.W. Sing, Adsorption, Surface Area, and Porosity, Academic Press, New York, 1982.
[34] D. Myers, Surfaces, Interfaces, and Colloids: Principles and Applications, Wiley-VCH, NewYork, 1999.
[35] H.P. Boehm, Surface oxides on carbon and their analysis: a critical assessment, Carbon 40 (2002) 145–149.
[36] M. Cristina, M. Almeida, L.V. Boas, Analysis of BTEX and other substituted benzenes in water using headspace SPME-GC-FID: method validation, J. Environ. Monitor. 6 (2004) 80–88.
[37] K.A. Wepasnick, B.A. Smith, K.E. Schrote, H.K. Wilson, S.R. Diegelmann, D.H. Fairbrother, Surface and structural characterization of multi-walled carbon nanotubes following different oxidative treatments, Carbon 49 (2011) 24–36.
[38] Y.C. Chiang, C.C. Lee, C.Y. Lee, Surface characterization of acid-oxidized multi-walled carbon nanotubes, Toxicol. Environ. Chem. 91 (2009) 1413–1427.
[39] Z.Z. Zhu, Z. Wang, H.L. Li, Functional multi-walled carbon nanotube/polyaniline composite films as supports of platinum for formic acid electrooxidation, Appl. Surf. Sci. 254 (2008) 2934–2940.
[40] W. Davis, C.L. Erickson, C.T. Johnston, Quantitative fourier transform infrared spectroscopic investigation humic substance functional group composition, Chemosphere 38 (1999) 2913–2928.
[41] A.A.M. Daifullah, B.S. Girgis, Impact of surface characteristics of activated carbon on adsorption of BTEX, Colloid Surface A 214 (2003) 181–193.
[42] L.A. Hoferkamp, E.J. Weber, Nitroaromatic reduction kinetics as a function of dominant terminal electron acceptor processes in natural sediments, Environ. Sci. Technol 40 (2006) 2206–2212.
[43] N. Wibowo, L. Setyadhi, D. Wibowo, J. Setiawan, S. Ismadji, Adsorption of benzene and toluene from aqueous solutions onto activated carbon and its acid and heat treated forms: influence of surface chemistry on adsorption, J. Hazard. Mater. 146 (2007) 237–242.
[44] S.H. Kundu, Y.M. Wang, W.X. Muhler, Thermal stability and reducibility of oxygen-containing functional groups on multiwalled carbon nanotube surfaces: a quantitative high-resolution XPS and TPD/TPR study, J. Phys. Chem. C 112 (2008) 16869–16878.
[45] M.Q. Tran, C. Tridech, A. Alfrey, A. Bismarck, M.S.P. Shaffer, Thermal oxidative cutting of multi-walled carbon nanotubes, Carbon 45 (2007) 2341–2350.
[46] V. Datsyuk, M. Kalyva, K. Papagelis, J. Parthenios, D. Tasis, A. Siokou, I. Kallitsis, C. Galiotis, Chemical oxidation of multiwalled carbon nanotubes, Carbon 46 (2008) 833–840.
[47] R.M. Allen-King, P. Grathwohl, W.P. Ball, New modeling paradigms for the sorption of hydrophobic organic chemicals to heterogeneous carbonaceous matter in soils, sediments, and rocks, Adv. Water Resour. 25 (2002) 985–1016.
[48] J.J. Pignatello, B. Xing, Mechanisms of slow sorption of organic chemicals to natural particles, Environ. Sci. Technol. 30 (1996) 1–11.
[49] Y.S. Ho, G. McKay, Sorption of dye from aqueous solution by pit, Chem. Eng. J. 70 (1998) 115–124.
[50] Y.S. Ho, G. McKay, Pseudo-second order model for sorption processes, Process Biochem. 34 (1999) 451–465.
[51] Q. Yu, R.Q. Zhang, S.B. Deng, J. Huang, G. Yu, Sorption of perflurooctane sulfonate and perfluorooctanoate on activated carbons and resin: kinetics and isotherms study, Water Res. 43 (2009) 1150–1158.
[52] F. Villacanas, M.F.R. Pereira, J.J.M. Orfao, J.L. Figueiredo, Adsorption of simple aromatic compounds on activated carbons, J. Colloid Interface Sci. 293 (2006) 128–136.
[53] C.J.M. Chin, M.W. Shih, H.J. Tsai, Adsorption of nonpolar benzene derivatives on single-walled carbon nanotubes, Appl. Surf. Sci. 256 (2010) 6035–6039.
[54] X.L. Wang, Y. Liu, S. Tao, B.S. Xing, Relative importance of multiple mechanisms in sorption of organic compounds by multiwalled carbon nanotubes, Carbon 48 (2010) 3721–3728.